NPP PRIMARY HEAT TRANSPORT CIRCUIT HEAT-UP RATE COMPUTING, FROM COLD SHUTDOWN STATE

Constantin NEAGA[1], Radu Bogdan ISTRATE[2]

Lucrarea de față propune un model matematic de calcul pentru determinarea vitezei optime de încălzire a circuitului primar dint-o CNE, plecând de la ideea că într-o CNE colectoarele de intrare, respectiv de ieşire ale reactorului sunt componentele structurale cele mai „sensibile" la funcționarea în regimuri tranzitorii. Analiza şi interpretarea rezultatelor obținute în coroborare cu proprietățile mecanice ale metalului colectoarelor, oferă specialiştilor în mod expres, găsirea vitezei de pornire a CNE – prin subansamblurile ei esențiale, colectoarele reactorului. Valorile de calcul obținute în urma simulărilor numerice sunt prezentate pentru cazul concret al unei CNE Candu 600.

The present paper proposes a mathematical model in order to determine the optimum heat-up rate for NPP Primary Heat Transport Circuit, based on the assumption that the reactor inlet and outlet headers are the most "sensitive" structures during thermal transitory regimes. The analysis and the interpretation of the data obtained from the calculus combined with the mechanical properties of headers material, offers to technical specialists the finding of the NPP heat-up rate based on the essential equipments, reactor headers. Numerical simulation results are presented for a Candu 600 NPP.

Keywords: transitory phase, thermomechanical stress, heat-up rate optimization.

1. Introduction

The Primary Heat Transport Circuit heat-up rate for a Nuclear Power Plant (NPP) dictates the overall power plant start-up speed and hence, it determines the time frame between cold start-up and power delivery to the national grid. This time frame is called the start-up time. Due to economic reasons it arises the need of plant start-up time shortage which further implies the optimum heat-up rate determination, while satisfying all the safety rules for the thermomechanical equipment implied.

Some of the vital equipment part of NPP primary circuit are the reactor inlet and outlet headers, thick metallic wall equipments, under internal pressure of reactor coolant.

[1] Professor, Mechanical Engineering and Mechatronics Faculty, University POLITEHNICA of Bucharest, Romania
[2] PhD Student, Mechanical Engineering and Mechatronics Faculty, University POLITEHNICA of Bucharest, Romania, email: istratebogdan@yahoo.com

Due to their particular design features, the thick wall header suffers significant thermal stresses during any thermal transitory phase, like for example the start-up from the cold state.

By not correlating the plant start-up speed with the acceptable header heat-up rate, material flaws it may result. This kind of damages will imply large economic penalties for repairs and nevertheless, for the extended outage time when the plant is not able to deliver power to the grid.

Header heat-up rate equation presented in this paper contains all the relevant terms implied in the transitory phase, allowing the analysis of various methods for improving the heat-up process.

The physical model of the primary circuit is presented in Fig. 1, [8]. The inlet headers, outlet headers respectively, (4) and (5), deliver or collect the heavy water which circulates through the reactor core (2), removing heat generated within the fuel. The primary circuit heat-up is based on the heat introduced by the coolant circulation pump (3) and by the heat developed within the nuclear fuel. The heat-up rate is observed and maintained constant during all the time frame considered.

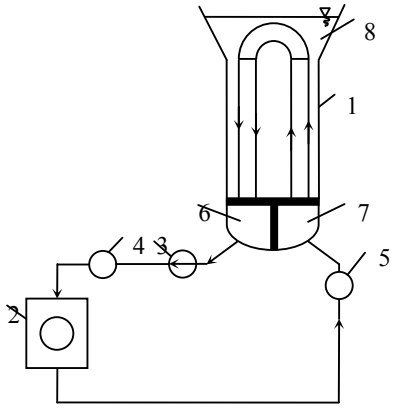

Fig. 1 NPP schematic diagram

1 – steam generator (SG), 2 – nuclear reactor, 3 – coolant circulation pump, 4 – inlet header, 5 – outlet header, 6 – SG outlet waterbox, 7 – SG inlet waterbox, 8 – SG secondary side.

In principle, reactor headers are cylindrical equipments, provided with elliptical welded end caps, thick walls, internal pressure, horizontal axis, with nozzles for coolant circulation through individual pipes. For a Candu 600 there are 95 nozzles for each header, having diameters varying in range of 60 mm to 100 mm. The nozzles are arranged on the cylinder element, in a square lattice. The header is made of carbon steel. The thermal expansion is not prevented.

2. Temperature fields in the header wall

A first necessary step to determine the header heat-up rate is the finding of temperature field variation in the header wall during a transitory phase, such as the plant start-up. To develop the relations which lead to temperature field determination, the following hypotheses were utilized:

a. the header warm-up takes place from the inside, from the coolant, with a constant rate through all the transitory phase considered;
b. the metal temperature varies only in radial direction. The metal temperature is constant in axial and tangential axis;
c. the coolant flow is subcooled, single phase, through all the transitory phase considered;
d. the header external surface is considered as perfectly insulated; this means that no heat transfer with the surroundings exists;
e. there are no internal heat generation sources within the header wall;
f. the coolant flow rate through the header is constant through all the transitory phase considered;
g. the header wall thickness is constant;
h. the material characteristics which are used to compute the thermal fields are considered variable with the metal temperature through the analyzed domain.

The expression of axial symmetrical thermal conduction through a cylindrical wall, without holes, without internal heat generation sources, in one dimension, for a transitory phase – cylindrical coordinates is, [1]:

$$\frac{\partial t}{\partial \tau} = a\left(\frac{\partial^2 t}{\partial r^2} + \frac{1}{r}\frac{\partial t}{\partial r}\right), \tag{1}$$

where t - header metal temperature, function of time and space, $t(\tau, r)$, °C; r - header radius, m; τ - time, s; a - metal thermal diffusivity, $a = \lambda/(\rho c_p)$, m^2/s; λ - metal thermal conductivity, function of temperature, W/(m·K); ρ - header metal density, function of temperature, kg/m^3; c_p - header metal specific heat, function of temperature, J/(kg·K).

Taking into consideration the significance of the term $\partial t/\partial \tau$, °C/s, metal temperature variation speed in time, or in the other words metal heat-up rate, and assigning the notation h_r, °C/s to this term, the equation (1) is written simplified:

$$h_r = a\left(\frac{\partial^2 t}{\partial r^2} + \frac{1}{r}\frac{\partial t}{\partial r}\right). \tag{1'}$$

Assuming that h_r is constant in the radial direction, equation (1') will have a solution of the following form:

$$t(r)=\frac{h_r}{4a}r^2+C_1\ln r+C_2. \tag{2}$$

To determine the integration constants C_1 and C_2 the boundary conditions should be written:

a) for $r=r_i$ the temperature is $t=t_i$; equation (2) becomes:

$$t(r_i)=t_i=\frac{h_r}{4a}r_i^2+C_1\ln r_i+C_2; \tag{2'}$$

b) in order to obtain the second boundary condition, the energy balance equation should be established between the conduction heat flux received by a mass element from the metal wall and the increase in the energy of the element during infinite small time, $d\tau$:

$$-2\pi r_i dl\lambda\left.\frac{dt}{dr}\right|_{r=r_i}=\int_{r_i}^{r_e}\frac{d}{d\tau}\left(2\pi r dl\rho c_p t\right)dr. \tag{2''}$$

The integration constants C_1 and C_2 are calculated as:

$$C_1=-\frac{h_r}{2a}r_e^2;\ C_2=t_i-\frac{h_r}{4a}r_i^2+\frac{h_r}{2a}r_e^2\ln r_i. \tag{2'''}$$

Replacing C_1 and C_2 in equation (2) the temperature distribution equation in the header wall is obtained:

$$t(r)=t_i+\frac{h_r}{4a}\left(r^2-r_i^2\right)-\frac{h_r}{2a}r_e^2\left(\ln r-\ln r_i\right)\ \text{or}\ t(r)=t_i+\frac{h_r}{4a}\left[\left(r^2-r_i^2\right)-2r_e^2\ln\frac{r}{r_i}\right]. \tag{3}$$

where r is the current header radius, r_i and r_e internal radius, external header radius respectively, in meters, $r_i\le r\le r_e$, Figure 2.

It is important to highlight that the header wall temperature distribution is a function of space, r coordinate, as well as a function of time, through h_r °C/s.

The internal surface metal wall temperature t_i will be determined by the thermal balance equation written for the metal wall which is warmed by the heat flux from the coolant agent which circulates inside the header. The header is assumed filled with water:

$$2\pi r_i\alpha_{hw}\left(t_{hw}-t_i\right)=\int_{r_i}^{r_e}\frac{d}{d\tau}\left(2\pi r\rho c_p t\right)dr=2\pi\rho c_p h_r\int_{r_i}^{r_e}r dr, \tag{4}$$

where:

t_{hw} - heavy water temperature, variable in time, °C; α_{hw} - convection heat transfer coefficient from heavy water to metal wall, W/(m^2·K). The temperature t_i variation equation becomes:

$$t_i=t_{hw}-\frac{\rho c_p h_r\left(r_e^2-r_i^2\right)}{2r_i\alpha_{hw}}. \tag{5}$$

Finally, the equation which describes the temperature fields inside the metal wall (3), as a function of time τ , space r and coolant temperature t_{hw}, can be expressed as:

$$t(r,\tau)=t_{hw}-\frac{\rho c_p h_r\left(r_e^2-r_i^2\right)}{2r_i\alpha_{hw}}+\frac{h_r}{4a}\left(r^2-r_i^2\right)-\frac{h_r}{2a}r_e^2\left(\ln r-\ln r_i\right), \tag{6}$$

Convection heat transfer coefficient from heavy water to metal wall can be determined using the relation developed by Gnielinski [13] for turbulent flow:

$$Nu=\frac{(\xi/8)\,\mathrm{Re}\,\mathrm{Pr}}{1+12.7\sqrt{\xi/8}\left(\mathrm{Pr}^{2/3}-1\right)}\left[1+\left(\frac{d_i}{l}\right)^{2/3}\right],$$

where d_i - inner header diameter, m; l - header length, m; Re,Pr - Reynolds, Prandtl numbers; $Nu=\alpha_{hw}d_i/\lambda_{hw}$, $\mathrm{Re}=wd_i/\nu_{hw}$, $\mathrm{Pr}=\nu_{hw}/a_{hw}$; a_{hw} - water thermal diffusivity, m^2/s; λ_{hw} - water thermal conductivity, W/(m·K); w - water velocity flowing inside the header, m/s; ν_{hw} - water kinematic viscosity, m^2/s; ξ - the friction factor for turbulent flow in smooth pipes, determined by Konakov [10, 11]; $\xi=\left(1.8\log_{10}\mathrm{Re}-1.5\right)^{-2}$. The water properties are defined for the average temperature within the heat-up range considered in the analysis.

3. Thermomechanical stress inside the header wall

Fig. 2 presents a section through the header wall.

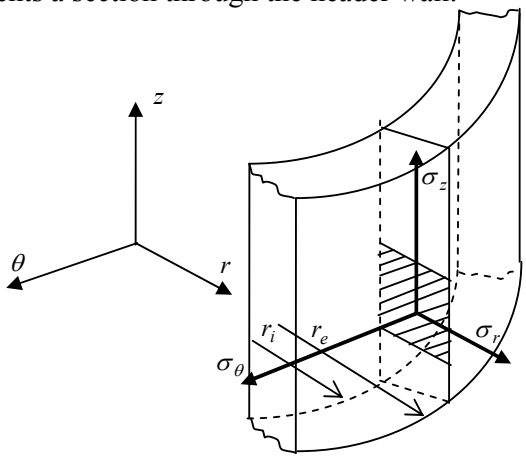

Fig. 2 Stresses in the header cylindrical wall

In order to develop the relations which will lead later to header wall thermomechanical stresses equations, the following hypothesis were made:

a. the header material is elastic, homogenous and isotropic; Hooke's law actions unlimited;
b. thermal expansion is not obstructed;

c. Saint-Vénant principle is valid through the investigated area;
d. the resultant loadings are in the elastic range;
e. the header is under internal pressure due to coolant agent. There is no external pressure influence;
f. the coolant pressure is considered constant, without oscillations, during the transitory phase considered in this paper;
g. the mechanical influences by the piping connected to the header are not considered.

The strength calculus which follows take care of thermal stresses and mechanical stresses which action together on the header. Algebraic summing of these stresses leads to the final equation whose solution represents the header heat-up rate and hence it yields to finding of the safe circuit heat-up rate.

3.1 Stresses due to the internal pressure

Mechanical stresses developed within the metal wall are only due to the internal coolant pressure. First, the wall without holes and nozzles is considered. The following equations don't take into account the fluid weight and the reaction forces between piping and header are neglected.

The mechanical stresses within metal wall $\sigma_r(p)$, $\sigma_\theta(p)$ and $\sigma_z(p)$, for a thick wall cylinder [2, 3, 5] are written as:

- radial coordinate:

$$\sigma_r(p)=\frac{r_i^2 p}{r_e^2-r_i^2}\left(1-\frac{r_e^2}{r^2}\right),\ \text{or}\ \sigma_r(p)=-p\frac{\beta_r^2-1}{\beta^2-1}; \tag{7}$$

- tangential coordinate:

$$\sigma_\theta(p)=\frac{r_i^2 p}{r_e^2-r_i^2}\left(1+\frac{r_e^2}{r^2}\right),\ \text{or}\ \sigma_\theta(p)=p\frac{\beta_r^2+1}{\beta^2-1}; \tag{8}$$

- axial coordinate:

$$\sigma_z(p)=\frac{r_i^2 p}{r_e^2-r_i^2},\ \text{or}\ \sigma_z(p)=p\frac{1}{\beta^2-1}; \tag{9}$$

where p - coolant pressure, MPa; $\beta_r=r_e/r$ and $\beta=r_e/r_i$, header radius ratio.

Analyzing the equations (7), (8) and (9) it can be concluded that:

$$\sigma_r(p)<\sigma_z(p)<\sigma_\theta(p)\ \text{and}\ \sigma_\theta(p)-\sigma_z(p)=\sigma_z(p)-\sigma_r(p)=\frac{\sigma_\theta(p)-\sigma_r(p)}{2}. \tag{10}$$

Since at constant pressure the mechanical stresses within the wall depends on variable r, header radius, it is useful to represent it graphically, Figure 3. Stress $\sigma_\theta(p)$ reaches a maximum at the header inner surface, $r=r_i$ and takes the value $\sigma_\theta(p)=\frac{r_e^2+r_i^2}{r_e^2-r_i^2}p=p\frac{\beta^2+1}{\beta^2-1}$.

Remind that all the above relations are written for the wall without holes in it. The presence of holes in the header wall weakens the mechanical strength. They epresent stress concentrators. Due to this reason, to better approximate the real model, it is necessary to introduce a stress concentration factor around the holes, due to internal pressure. Its symbol is c_θ and can be taken from the literature [13, 14]. The stress concentration factor depends on various parameters, especially geometric ones: cylinder shape, holes arrangement, cylinder diameter and holes diameter.

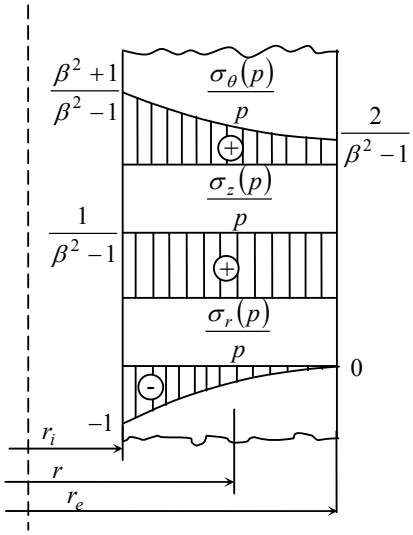

Fig. 3 Mechanical stress distribution within the header wall

3.2 Thermal stress within the header wall

Thermal stresses within metal wall arise due to transverse temperature distribution along the thickness of the wall (temperature between layers is different). During the heat-up, on the inner face, compression stresses develop due to expansion that doesn't proceed freely between the material layers. The external layers are under tension stresses (it is illustrated by the below equations).

Thermal stress within the metal header wall $\sigma_r(t)$, $\sigma_\theta(t)$ and $\sigma_z(t)$, for a cylindrical shape, are [2, 3, 9]:

$$\sigma_r(t)=\frac{\alpha E}{1-\nu}\left[\frac{r^2-r_i^2}{r^2\left(r_e^2-r_i^2\right)}\int_{r_i}^{r_e} rt(r)dr-\frac{1}{r^2}\int_{r_i}^{r} rt(r)dr\right];$$

$$\sigma_\theta(t)=\frac{\alpha E}{1-\nu}\left[\frac{r^2+r_i^2}{r^2\left(r_e^2-r_i^2\right)}\int_{r_i}^{r_e} rt(r)dr+\frac{1}{r^2}\int_{r_i}^{r} rt(r)dr-t(r)\right]; \tag{11}$$

$$\sigma_z(t)=\frac{\alpha E}{1-\nu}\left[\frac{2}{\left(r_e^2-r_i^2\right)}\int_{r_i}^{r_e} rt(r)dr-t(r)\right],$$

where E - modulus of elasticity in tension and compression, temperature dependant, MPa; α - linear thermal expansion coefficient, temperature dependant, 1/K; ν - Poisson's ratio; $t(r)$ - temperature distribution law within the wall, as a function of radius, °C.

Figure 2 presents, in cylindrical coordinates system, the three stresses $\sigma_r(t)$, $\sigma_\theta(t)$ and $\sigma_z(t)$.

Replacing the thermal distribution equation (3) in thermal stress relations (11) for each of the radii $r=r_i$ and $r=r_e$ the final form is obtained:

- radial coordinate:

$$\sigma_r(t)\big|_{r=r_i}=0;\ \ \sigma_r(t)\big|_{r=r_e}=0; \tag{12}$$

- tangential coordinate:

$$\sigma_\theta(t)\big|_{r=r_i}=\frac{\alpha E}{(1-\nu)a}h_r h^2\phi_i; \tag{13}$$

$$\sigma_\theta(t)\big|_{r=r_e}=\frac{\alpha E}{(1-\nu)a}h_r h^2\phi_e; \tag{14}$$

where h - wall thickness, $h=r_e-r_i$, m; ϕ_i and ϕ_e are the header shape factors, described by:

$$\phi_i=\frac{1}{8}\frac{\left(\beta^2-1\right)\left(3\beta^2-1\right)-4\beta^4\ln\beta}{\left(\beta^2-1\right)(\beta-1)^2};\ \ \phi_e=\frac{1}{8}\frac{\left(\beta^4-1\right)-4\beta^4\ln\beta}{\left(\beta^2-1\right)(\beta-1)^2};$$

- axial coordinate:

$$\sigma_z(t)\big|_{r=r_i}=\sigma_\theta(t)\big|_{r=r_i}; \tag{15}$$

$$\sigma_z(t)\big|_{r=r_e}=\sigma_\theta(t)\big|_{r=r_e}. \tag{16}$$

It can be observed that the maximum thermal stress occurs at the inner surface or at the external surface of the header, being equal in both axial and tangential directions, equations (13) to (16). Graphical variation of thermal stresses is presented below in Fig. 4.

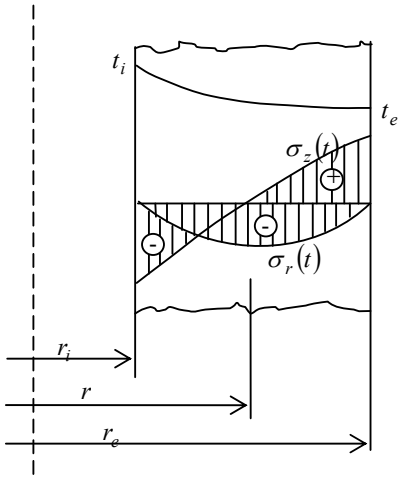

Fig. 4 Thermal stress distribution within the header wall

All the above relations are written for the wall without holes in it. Like for the mechanical stress equations development, the introduction of a stress concentration factor is required. Its symbol is c_t and it is taken from the literature. The factor is determined for a plane plate with a hole, under a thermal gradient and not allowed to free expanding.

If in (13) to (16) the geometric constants are separated by the material properties, and assigning the notation: $C_m = \frac{\alpha E}{(1-\nu)a}$ and $C_g = h^2 \phi_{i/e}$ it is obtained:

$$\sigma_\theta(t)\big|_{r=r_i} = \sigma_z(t)\big|_{r=r_i} = h_r c_t C_m C_g;\ \ \sigma_\theta(t)\big|_{r=r_e} = \sigma_z(t)\big|_{r=r_e} = h_r c_t C_m C_g. \tag{17}$$

From (17) it can be concluded that the thermal stresses $\sigma_z(t)$ and $\sigma_\theta(t)$, for a cylinder, at a given dimensions and material, at a certain temperature, vary proportional with the heat-up rate h_r.

4. Heat-up rate for the header wall

As stated previously, it is clear that the stress in a random point inside the header wall is defined by the mechanical stress due to the internal pressure $\sigma(p)$, and thermal stress due to thermal fields through the header wall thickness during the transitory phase of heat-up, $\sigma(t)$.

Regarding the strength theories developed by strength of materials studies [2, 3, 4], certain relationships are established between stress inside a body and the moment when failure is achieved, in the other words, when the stress within the header material reaches the yield stress. A factor of safety, which takes care about the working temperature, is considered.

For the particular header case, the principal stresses in any point inside the structure are obtained by algebraically summing of the thermal and the mechanical stresses, in the three coordinates z, θ and r:

$$\sigma_z(t,p)=\sigma_z(t)+\sigma_z(p),\ \ \sigma_\theta(t,p)=\sigma_\theta(t)+\sigma_\theta(p),\ \ \sigma_r=\sigma_r(t)+\sigma_r(p). \tag{18}$$

The equivalent stress is computed using Tresca's theory (the III-rd strength theory) which is the maximum shear stress theory. This theory states that failure occurs when the maximum shear stress in the component being analyzed equals the maximum shear stress in a uniaxial tensile test at the yield stress. Tresca's criterion is one of the two main failure criteria used today. The second important criterion is due to von Mises, the V-th strength theory. Tresca's theory predicts plastic yielding already for stress states that are still elastic according to the von Mises criterion. As a model for plastic material behavior, Tresca's criterion is therefore more conservative.

Anyway, Tresca's criterion is applied in ASME Boiler and Pressure Code which is the basis for design of American NPPs (including CANDU) [12].

Knowing the principal stresses σ_1, σ_2 and σ_3 and arranging in order of magnitude, then the equivalent stress is the difference between the greatest and the lowest value:

$$\sigma_{ech}=\sigma_1-\sigma_3. \tag{19}$$

The first step is to determine the following differences, for $r=r_e$ and $r=r_i$:

$$\max\left[\sigma_z(t,p)-\sigma_\theta(t,p);\sigma_\theta(t,p)-\sigma_r(t,p);\sigma_r(t,p)-\sigma_z(t,p)\right] \tag{20}$$

After developing the differences and replacing in (19) it is obtained:

a. Principal stress for $r=r_i$:

$$\begin{aligned}
&\sigma_\theta(t,p)-\sigma_z(t,p)=p\left(c_\theta\frac{\beta^2+1}{\beta^2-1}-\frac{1}{\beta^2-1}\right);\\
&\sigma_\theta(t,p)-\sigma_r(t,p)=p\left(c_\theta\frac{\beta^2+1}{\beta^2-1}+1\right)+\frac{\alpha E}{(1-\nu)a}h_r c_t h^2\phi_i;\\
&\sigma_z(t,p)-\sigma_r(t,p)=p\left(\frac{1}{\beta^2-1}+1\right)+\frac{\alpha E}{(1-\nu)a}h_r c_t h^2\phi_i.
\end{aligned} \tag{21}$$

b. Principal stress for $r=r_e$:

$$\begin{aligned}
&\sigma_\theta(t,p)-\sigma_z(t,p)=p\left(c_\theta\frac{2}{\beta^2-1}-\frac{1}{\beta^2-1}\right);\\
&\sigma_\theta(t,p)-\sigma_r(t,p)=p\left(c_\theta\frac{2}{\beta^2-1}\right)+\frac{\alpha E}{(1-\nu)a}h_r c_t h^2\phi_e;\\
&\sigma_z(t,p)-\sigma_r(t,p)=p\left(\frac{1}{\beta^2-1}\right)+\frac{\alpha E}{(1-\nu)a}h_r c_t h^2\phi_e.
\end{aligned} \tag{22}$$

Solving the above equations the allowable heat-up rate is obtained. It can be seen that the heat-up rate depends on: the internal fluid pressure, the equivalent stress σ_{ech} which is temperature dependant (it decreases with increasing temperature), geometric parameters (header radius, wall thickness), physical material properties, the layout of nozzles and their dimensions.

5. Numerical analyses. Graphical representation. Interpretation

5.1 Temperature fields within the wall

Equation (6) which was obtained in the second paragraph leads to finding the temperature field within the wall for different heat-up rates. The initial coolant temperature is considered 40 °C and the warm-up phase is considered complete after achieving 260 °C. Any subsequent temperature increase up to 310 °C is due to reactor power increasing. This last period is not covered in this paper.

Since saturation at 260 °C is reached at 4.5 MPa, in order to avoid the coolant boiling, during the warm-up the pressure must be greater than 5.0 MPa. The nominal pressure and hence the maximum pressure possible for the warm-up is 10.0 MPa. Considering these statements, the heat-up rates were determined for pressure, temperature ranges: 5.0 MPa ÷ 10.0 MPa, 40 °C ÷ 260 °C.

The header material is carbon steel SA 106 Gr.B.

In equation (6) there are a series of physical parameters which are temperature dependant and were approximated by second degree polynomial functions:

- metal thermal conductivity: $\lambda(t) = 52.353 - 0.0172 \cdot t - 3 \cdot 10^{-5} \cdot t^2$, W/(m·K);
- header metal density: $\rho(t) = 7883{,}167 - 0.2922668 \cdot t - 1.066654 \cdot 10^{-4} \cdot t^2$, kg/m^3;
- header metal specific heat: $c_p(t) = 429.82 + 0.5523 \cdot t - 0.0004 \cdot t^2$, J/(kg·K).

For finding α_{hw}, (convection heat transfer from coolant to cylindrical header wall, W/(m^2·K)), the water physical parameters were determined at the average temperature in the considered range: water thermal conductivity $\lambda_{hw} = 0.6882$, W/(m·K); water kinematic viscosity $\nu_{hw} = 0.2001 \cdot 10^{-6}$, m^2/s; water density $\rho_{hw} = 920.67$, kg/m^3; water specific heat $c_{p\,hw} = 4290$, J/(kg·K). Finally, it was obtained the convection heat transfer coefficient $\alpha_{hw} = 8539$, W/ (m^2·K).

5.2 Thermomechanical stresses within the header wall

In order to calculate the thermomechanical stresses the following temperature dependant second degree polynomial functions were used:

- Young modulus: $E(t) = 204483 - 62.589 \cdot t - 0.0065 \cdot t^2$, MPa;

- linear thermal expansion coefficient: $\alpha(t) = 10.769 + 0.0078 \cdot t - 2 \cdot 10^{-6} \cdot t^2$, [mm/(mm·°C)] 10^{-6};
- yield stress: $\sigma_y(t) = 249.54 - 0.3032 \cdot t + 0.0004 \cdot t^2$, MPa.

All the above relations are valid for the temperature range 20 °C ÷ 350 °C. This range covers totally the warm-up range 40 °C ÷ 260 °C, analyzed here.

Other parameters, not temperature dependant are: Poisson's ratio: $\nu = 0.3$; header geometric characteristics: $h = 0.07$ m, $\beta = 1.35$; shape factors: $\phi_i = -0.388$; $\phi_e = 0.166$.

Based on geometric structure, and more specific based on the header and the nozzles diameter, the stress concentration factors were chosen using the literature [15, 16]. It was determined $c_\theta = 3.5$. To determine the equivalent stress σ_{ech} it was preferred a high safety coefficient $c_s = 1.8$.

5.3 Results

From the allowable warm-up range, there were picked up three pressure values for heat-up rate computing, 5.0 MPa, 7.5 MPa and 10 MPa. The heat-up rate evolution over the temperature range is represented graphically in Figs. 5 to 8, for areas were the stresses were determined (header inners and outer surface).

Analyzing Fig. 5, it can be observed that the maximum heat-up rate is achieved on the external header surface, for the minimum coolant pressure, 5.0 MPa. At this value, the heat-up rate is imposed on the inner surface of the header. When pressure increases, the heat-up rate is imposed on external surface data.

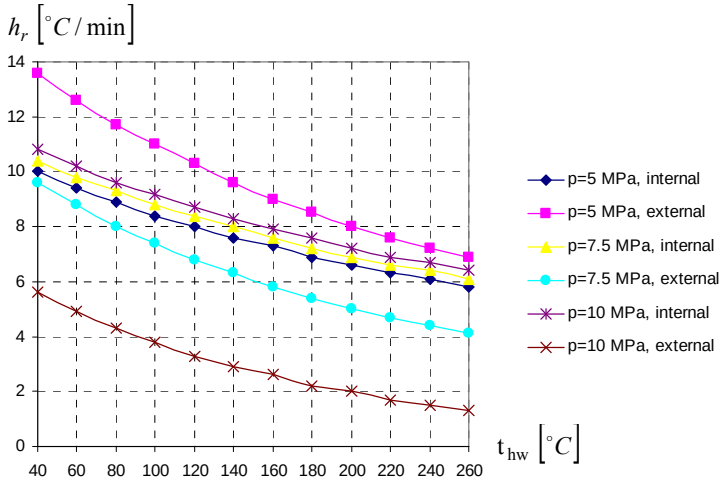

Fig. 5 Heat-up rate evolution for coolant pressure 5.0 MPa, 7.5 MPa, 10 MPa

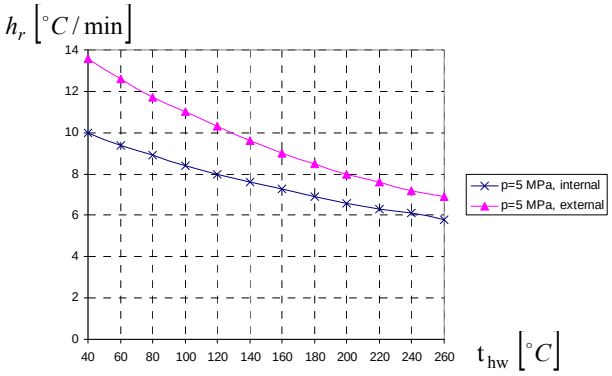

Fig. 6 Heat-up rate evolution for coolant pressure 5.0 MPa

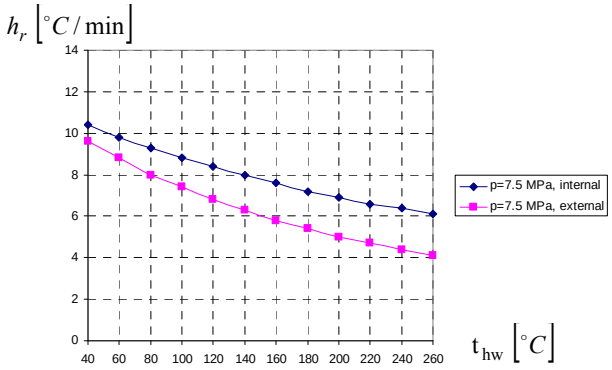

Fig. 7 Heat-up rate evolution for coolant pressure 7.5 MPa

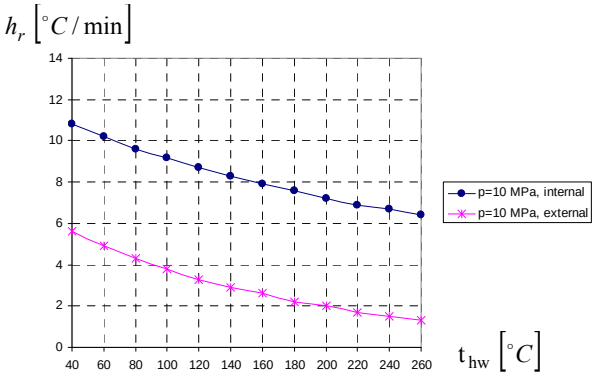

Fig. 8 Heat-up rate evolution for coolant pressure 10.0 MPa

In this way, it can be defined the inversion pressure which separates two different areas who impose the heat-up rate: first area up to 6.0 MPa, the heat-up rate is dictated by the internal surface of the header and the second one, above 6.0 MPa where heat-up rate is imposed on header external surface.

Figure 9 represents the heat-up rate evolution under the pressure range 5.0 MPa ÷ 10.0 MPa and fixed temperature value of 260 °C (the highest the temperature, the lower the heat-up rate). Figure 9 is useful in observing the pressure inversion point. Figure 10 represents the heat-up rate at 6.0 MPa.

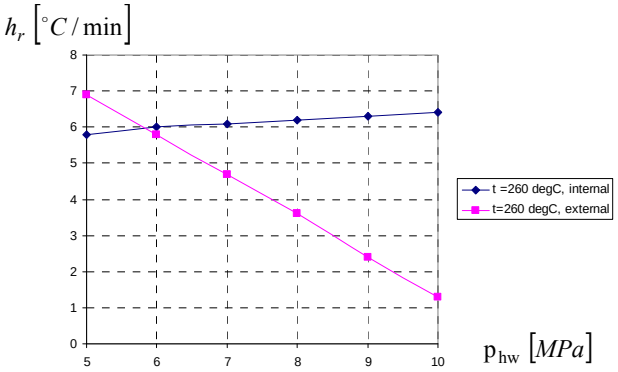

Fig. 9 Heat-up rate evolution for 260 °C, pressure range 5.0 MPa ÷ 10.0 MPa

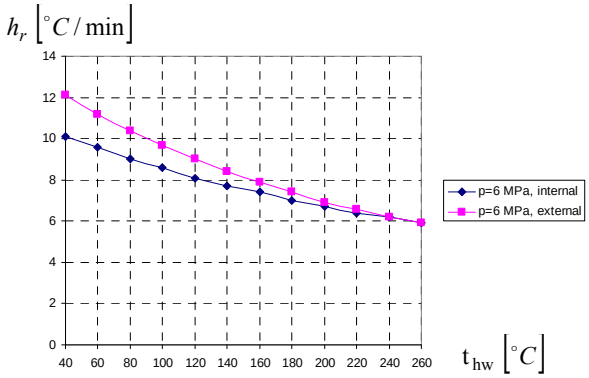

Fig. 10 Heat-up rate evolution for coolant pressure at inversion value 6.0 MPa

In Fig. 11 it was plotted, for 7.5 MPa coolant pressure, the heat-up rate evolution against equivalent stress along the range 40 °C ÷ 260 °C. For a decrease of approximate 17 % of equivalent stress, σ_{ech}, due to metal warming, a decrease of approximate 57 % of header heat-up rate is obtained.

Finally, to achieve the research objectives, the start-up time of the plant as a function of coolant pressure was plotted in Fig. 12. At each of coolant pressure value plotted, the heat-up rate was computed previously.

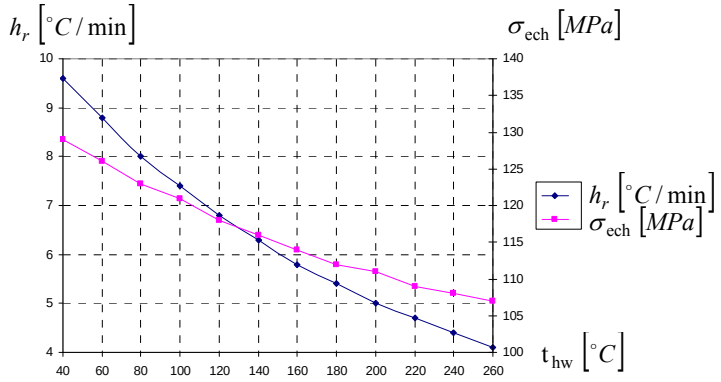

Fig. 11 Heat-up rate and equivalent stress evolution for 7.5 MPa

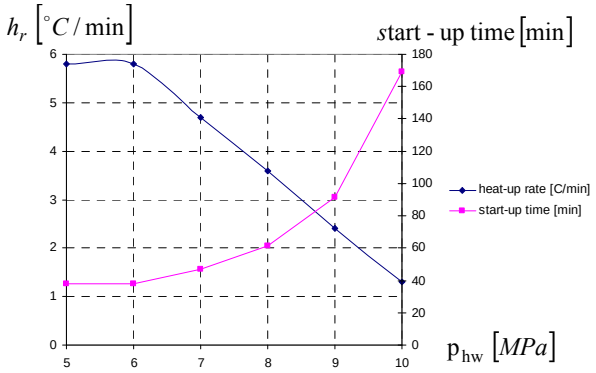

Fig. 12 Heat-up rate and start-up time evolution over range 5.0 MPa ÷ 10.0 MPa

6. Conclusions

- A complex mathematical model which defines the header heat-up rate was described. The model marks out the essential parameters which limit the heat-up rate. Those parameters can be split in two groups:

- geometrical and physical material parameters. This group is interesting in the design phase when it is possible to choose different characteristics which can improve the equipment response at various transients. During operation they could help in determining, with relative high accuracy, the allowable limits of the equipment;
- specific operational parameters (pressure, temperature, flow). This group is very important in equipment life time operation since different processes can be optimized, like for example the transitory phases of warm-up or cool-down.

- Despite the fact that some simplifying hypotheses were adopted, the mathematical model for the heat-up rate represents a safely method for determining and optimizing the functional parameters of the equipment.

- The heat-up rate is dictated by the coolant pressure, Fig. 5 to Fig. 10, and by the yield limit of the material which decreases with the temperature – Fig. 11.

- The recommended coolant pressure for all the heat-up phase in range 40 °C to 260 °C is approximate 7.5 MPa, where the heat-up rate is limited at 4 °C/min – Fig. 7. Lower coolant pressure allows higher heat-up rates, up to 6 °C/min., Fig. 6, but it could be dangerous for other mechanical equipments, like for example the possibility of circulating pumps cavitation. Higher pressure, up to 10 MPa, close to nominal pressure, decreases the heat-up rate to 1.5 °C/min, Fig. 8. In this case, the start-up time is increasing too much, Fig. 12.

- The results obtained are in line with operational practice of NPP and with the designer recommendations, approximate 3 °C/min.

R E F E R E N C E S

[1] *F. P. Incropera, D. P. DeWitt, T. L. Bergman, A. S. Lavine,* Fundamentals of Heat and Mass Transfer, Wiley, 2006
[2] *G. Buzdugan*, Strength of Materials, Ed. Tehnică, Bucureşti, 1974 (in Romanian)
[3] *S. Timoshenko, J. N. Goodier,* Theory of Elasticity, McGraw-Hill Book Company, 2nd Ed., 1951
[4] *S. Timoshenko,* Strength of Materials, Elementary Theory and Problems, D. Van Nostrand Company, 2nd Ed. 1940
[5] *S. Timoshenko* Theory of Plates and Shells, McGraw-Hill Book Company, 2nd Ed., 1959
[6] *C. Neaga, L. Cojocia*, "Heating Speed Calculus for Natural Circulation Steam Generator", in Energetica (45), **Vol. 8**, 1997, pp. 376-383 (in Romanian)
[7] *S Gheorghiu*, "Allowable Heating Rates for Natural Circulation Steam Generator", in Energetica (19), **Vol. 12**, 1971, pp. 573-581 (in Romanian)
[8] *C. Bratianu, V. Bendic, V. Georgescu*, Nuclear Energy Strategies and Nuclear Power Reactors, Ed. Tehnica, Bucuresti, 1990 (in Romanian)
[9] *M. Ceclan*, Tubular Heat Exchangers, Ed. Printech, Bucureşti, 2000 (in Romanian)
[10] *Dubbel*, Handbook of Mechanical Engineering, Fundamentals, Ed. Tehnica, Bucuresti, 1998
[11] *, VDI Heat Atlas, Second Edition, Springer, 2010
[12] *, ASME Boiler and Pressure Vessel Code, 1998
[13] *W. D. Pilkey*, Peterson's Stress Concentration Factors, Wiley, 3rd Ed., 2008
[14] *A. C. Ugural*, Advanced strength and applied elasticity, Prentice Hall PTR, 4th Ed, 2003